

Tuning the Location of Niobia/Carbon Composites in a Biphasic Reaction: Dehydration of D-Glucose to 5-Hydroxymethylfurfural

Haifeng Xiong · Tianfu Wang · Brent H. Shanks ·
Abhaya K. Datye

Received: 14 February 2013 / Accepted: 31 March 2013 / Published online: 10 April 2013
© Springer Science+Business Media New York 2013

Abstract The conversion of glucose to 5-hydroxymethylfurfural (HMF) was studied in a biphasic system with niobia solid acid catalysts. We used carbon supported niobia since it shows improved hydrothermal stability. However, the carbon supported catalysts tend to be located in the organic phase due to their hydrophobic nature, while the reactant glucose is present in the aqueous phase. Therefore, we functionalized the carbon black support to increase the degree of hydrophilicity, allowing us to locate the catalyst either in the organic phase, in the aqueous phase or at the interface. The effect of the location of the niobia/carbon composites on the catalytic performance was investigated in the conversion of D-glucose to HMF in a biphasic system. It was found that the niobia catalyst located in the aqueous phase showed the highest D-glucose conversion (twofold greater than the others). We also compared the performance of catalysts obtained by deposition of niobia on functionalized carbon with a catalyst prepared by deposition precipitation-carbonization (DPC). The latter catalyst provides crystalline niobia particles while the other catalysts yield amorphous niobia. The crystalline niobia is more active for the acid catalyzed dehydration of isopropanol in the vapor phase. The DPC method provides a simple one pot synthesis to generate niobia particles embedded in a carbon support.

Keywords Niobia/carbon acid catalyst · Biphasic reaction · Hydrophilic carbon · D-glucose conversion to 5-hydroxymethylfurfural

1 Introduction

5-hydroxymethylfurfural (HMF) has been suggested as an important biomass-derived chemical intermediate for the production of polymers, fine chemicals and transportation fuels [1–5]. The production of HMF from dehydration of D-glucose is a promising route because D-glucose is an abundant monosaccharide. The conversion of D-glucose to HMF carried out in a single phase (aqueous phase or ionic liquids [6, 7]) leads to a low HMF selectivity because HMF can undergo further reactions to form byproducts under the reaction conditions. Use of a biphasic system of two immiscible solvents (often water and a hydrophobic organic liquid), can avoid the aforementioned issue because HMF produced in the aqueous phase can migrate into the organic phase to avoid the further reaction [8]. Homogeneous Lewis acid catalysts have been extensively used in the conversion of D-glucose to HMF in biphasic reaction systems [9–11]. However, these homogeneous catalysts have several drawbacks including the production of waste, difficulty in separation from products and the recovery and reuse of the catalysts [12]. Thus, it is important to develop a heterogeneous acid catalyst for this reaction [13].

Recently, several studies have explored the use of heterogeneous catalysts in the conversion of glucose to HMF [9, 12–14]. For example, in conjunction with a Brønsted acid, tin-containing silica has been proved to catalyze the conversion of glucose [15]. In ionic liquid–water mixtures, ZrO₂ was found to promote the formation of HMF with the

H. Xiong · A. K. Datye (✉)
Department of Chemical and Nuclear Engineering and Center
for Micro-engineered Materials, University of New Mexico,
Albuquerque, NM 87131, USA
e-mail: datye@unm.edu

T. Wang · B. H. Shanks
Chemical and Biological Engineering, Iowa State University,
Ames, IA 50011, USA

addition of Cl^- or HSO_4^- anions [6]. Thus, it was noted that the addition of some salts or ions such as HCl , CrCl_2 or HSO_4^- can increase the yield of HMF. Without the additives, mesoporous TiO_2 nanospheres produced HMF with selectivity range from 4–30 % [14]. Typical solid acid catalysts are metal oxide based and they are not stable under hydrothermal conditions in the aqueous phase, leading to loss of surface area and reactivity [16]. Our recent findings indicated that carbon-loaded oxide composites show improved hydrothermal stability [17].

In general, pure carbon materials are hydrophobic [8, 18, 19], so, they partition into the organic phase in a biphasic reaction system. The hydrophobic surface of carbon materials can be tailored by introducing functional groups or oxides, so that the carbon materials could be located at the interface with the aqueous phase or within the aqueous phase. The different locations of carbon materials in a biphasic system can influence the performance of these catalysts, which is the focus of this study. We describe methods to tune the location of the carbon materials in biphasic solvents.

Niobium oxide is a solid acid catalyst that can be used extensively in important biomass reactions, such as dehydration, aldol condensation, hydrolysis and ketonization. Recently, pure bulk niobia was shown to be active for the dehydration of glucose to 5-(hydroxymethyl)furfural in the aqueous phase with a HMF yield of 20 % [12]. In this study, we generated nanostructured niobia/carbon composites whose properties were tailored for applications in biphasic reactions. By controlling the degree of functionalization, the niobia/carbon composites were located in different locations in the water/oil biphasic solvent system (water and *sec*-butyl phenol). The effect of catalyst location on the catalytic performance was investigated in the conversion of *D*-glucose to 5-hydroxymethylfurfural (HMF) in this biphasic system.

2 Experimental

2.1 Niobia/Carbon Catalyst Preparation

Nb/CB-DP Commercially-available carbon black (CABOT, Vulcan XC 72R) was pretreated in 50 % HNO_3 at 80 and 120 °C for 8 h, respectively. After filtration and washing by water till $\text{pH} = 7$, the obtained material was dried at 120 °C for 12 h and denoted as CB-1 and CB-2, respectively. Two niobia/carbon catalysts (nominally 10 wt% niobium loading) were prepared by homogeneous deposition precipitation (DP) using the pretreated carbon supports. Urea was used as the precipitating agent and the detailed synthesis route was as follows: ammonium niobium oxalate (0.41 g) and urea (0.27 g; 2.5 mol urea per mole of niobium) were dissolved in deionized water (250 mL) and added to 1 g of the

functionalized carbon black. Subsequently, the temperature was raised to 90 °C. After allowing sufficient time (17 h) for the hydrolysis of the urea, the sample was filtered and washed with deionized water, followed by drying at 100 °C for 10 h and calcining at 250 °C for 4 h in a flow of N_2 . The samples were denoted as Nb/CB-1-DP and Nb/CB-2-DP (CB stands for carbon black and DP stands for deposition precipitation).

Nb/CS-HT A niobia/carbon catalyst (nominal 10 wt% niobium loading) was prepared by a method we have called deposition precipitation-carbonization (DPC). The synthesis involved the use of 4 g of *D*-glucose dissolved in 250 mL deionized water and mixed with ammonium niobium oxalate (0.6724 g) and urea (0.2826 g). The mixture was placed in an autoclave and held at 200 °C for 12 h. The sample was pyrolyzed at 400 °C for 4 h in a flow of N_2 and denoted as Nb/CS-HT (CS stands for carbon spheres and HT stands for hydrothermal synthesis).

2.2 Catalyst Characterization

N_2 adsorption/desorption isotherms were recorded using a Quantachrome Autosorb-1 instrument. Prior to the experiment, the sample was out gassed at 200 °C for 6 h. The surface area was obtained using the BET method using adsorption data over a relative pressure range from 0.05 to 0.30. The total pore volumes were calculated from the amount of N_2 vapor adsorbed at a relative pressure of 0.99. Scanning electron microscopy (SEM) was performed on a Hitachi S-5200, with a resolution of 0.5 nm at 30 kV and 1.7 nm at 1 kV. Scanning transmission electron microscopy (STEM) was carried out in a JEOL 2010F microscope. The powders were deposited on holey carbon support films after being dispersed in ethanol. An electron probe, diameter of 0.2 nm, was scanned over the specimen, and electrons scattered at high angles were collected to form the images. The image contrast in the HAADF (high angle annular dark field) mode is atomic number dependent and is dependent also on the sample thickness in each pixel being imaged. Thermogravimetric analyses (TGA) was performed with a SDT Q600 TGA using nitrogen or air as the purge gas and a heating rate of 10 °C/min. The flow rate of purge gas was always 50 mL/min. Fourier transform infrared spectra (FTIR) were recorded on a Thermo Nicolet 6700 FTIR spectrometer, at a spectral resolution of 4 cm^{-1} , using 64 scans per spectrum.

2.3 Catalytic Activity and Hydrothermal Stability

2.3.1 Isopropanol Dehydration

Isopropanol dehydration was carried out in a fixed-bed flow reactor as a general probe of the acidic properties of the catalysts. A mass of ca. 20 mg of catalyst was used. The reactor

was purged by flowing ultra high purity (UHP) Ar (ca. 25 mL min⁻¹) for 30 min and then the temperature was increased to 180 °C. The reaction was performed at 180 °C and atmospheric pressure with Ar (ca. 25 mL min⁻¹) as carrier gas and isopropanol (0.002 mL min⁻¹) was pumped to the reactor by a HPLC pump (Eldex). Reactants and products were analyzed with an on-line GC (Varian 3800) equipped with a capillary column (Porapak-T) and a FID detector.

2.3.2 Conversion of Glucose to 5-Hydroxymethylfurfural (HMF)

A biphasic reaction system (water and sec-butyl phenol) was used to study the conversion of D-glucose to 5-hydroxymethylfurfural [20]. The mass ratio of sec-butyl phenol (SBP) solvent to water was 2:1. Here, SBP is an extracting solvent for HMF. The advantage of using SBP is that higher HMF yields can be obtained, as compared to other organic solvents such as tetrahydrofuran (THF), methyl isobutyl ketone (MIBK), and 2-butanol [20, 21]. The reaction was carried out in an Alltech reactor. 0.1 g catalyst was used and the reaction temperature is 170 °C and reaction time is 120 min. After reaction, liquid effluents were collected and compositions were quantified in a Waters 1525 HPLC system equipped with a 2998 PDA UV detector and a 2414 refractive index detector maintained at 60 °C. Aqueous phase samples were analyzed using a PL Hi-Plex H-form carbohydrate column at 80 °C, using 5 mM H₂SO₄ as the mobile phase at a flow rate of 0.6 mL min⁻¹. Organic phase samples were analyzed using a Zorbax SB-C18 reverse phase column (Agilent) at 35 °C, with a methanol:water (8:2 v/v) mixed solvent at a flow rate of 0.7 mL min⁻¹.

3 Results and Discussion

3.1 N₂ Physisorption

Table 1 displays the N₂ physisorption results for the niobia/carbon composites. As can be seen, all the niobia/carbon catalysts showed a surface area >100 m²/g. Compared to the as-received carbon black, the Nb/CB-2-DP and Nb/CB-1-DP samples show higher pore volumes as a result of the reaction with nitric acid at elevated temperatures. The increase in pore volume is due to the formation of macro pores due to the etching of the carbon, but this also leads to a loss of surface area from Nb/CB-1-DP to Nb/CB-2-DP likely due to a loss of the micropores.

3.2 Electron Microscopy

Figure 1 shows the TEM images of functionalized carbon black with different extents of nitric acid treatment (CB-1

and CB-2). As can be seen, the as-received carbon black shows spherical particles of graphitic carbon (Fig. 1a). After acid treatment at 80 °C we do not see much change in the morphology (Fig. 1b). High-resolution TEM shows that the carbon spheres are composed of curved graphitic sheets within the spherical particles (Fig. 1c). However, after acid treatment at 120 °C, the carbon black morphology changed significantly. The TEM images indicate that the primary particles are now hollow, which can explain the increased pore volume of the functionalized carbon (Fig. 1d). The observed hollow carbon black structure is a result of the poor degree of graphitization of the interior making it more susceptible to etching when the carbon is treated with nitric acid. The harsher acid treatment creates functional groups transforming the carbon surface from being hydrophobic to becoming hydrophilic so that the carbon can be easily dispersed in polar solvents, such as ethanol.

Representative SEM/STEM images of niobia/carbon catalysts prepared by deposition precipitation are shown in Fig. 2. The SEM image of Nb/CB-1-DP shows niobia particles with an average size of 20 nm dispersed on the carbon black surface (Fig. 1a). The STEM image shows that the niobia clusters of ca. 20 nm are actually composed of smaller niobia particles with an average size of 3 nm (Fig. 2b). The STEM image of Nb/CB-2-DP shows niobia clusters around 20 nm in diameter, hence there is no significant difference in niobia particle morphology (Fig. 2c) compared to Nb/CB-1-DP. The HR-TEM image of Nb/CB-2-DP shows that the niobia particles are amorphous (Fig. 2d, inset).

Representative SEM/STEM images of Nb/CS-HT prepared by the DPC method are shown in Fig. 3. The method has been described in more detail elsewhere [17]. As shown in Fig. 3a, the Nb/CS-HT composite shows a spherical morphology with a diameter of 20–50 nm. These spheres can be easily crushed yielding a powder that contains niobia particles with a size of ca. 8 nm (Fig. 3b). The high-resolution TEM image of Nb/CS-HT shows lattice fringes (Fig. 3b, inset) indicating that the niobia particles are crystalline, which is different from the amorphous niobia seen on both Nb/CB-1-DP and Nb/CB-2-DP. The synthesis of this catalyst involved a higher temperature (200 °C) under hydrothermal conditions (22 bar) which causes the niobia to become crystalline.

3.3 Fourier Transform Infrared Spectroscopy (FTIR)

Figure 4 shows the FTIR spectra of the three niobia/carbon catalysts. For Nb/CB-1-DP and Nb/CB-2-DP, two bands at 1,693 and 1,510 cm⁻¹ were observed in the FTIR spectra as well as an intense band at 1,800–2,600 cm⁻¹ (Fig. 4a, b). These are ascribed to the formation of functional

Table 1 BET surface area, pore volume of the niobia/carbon catalysts

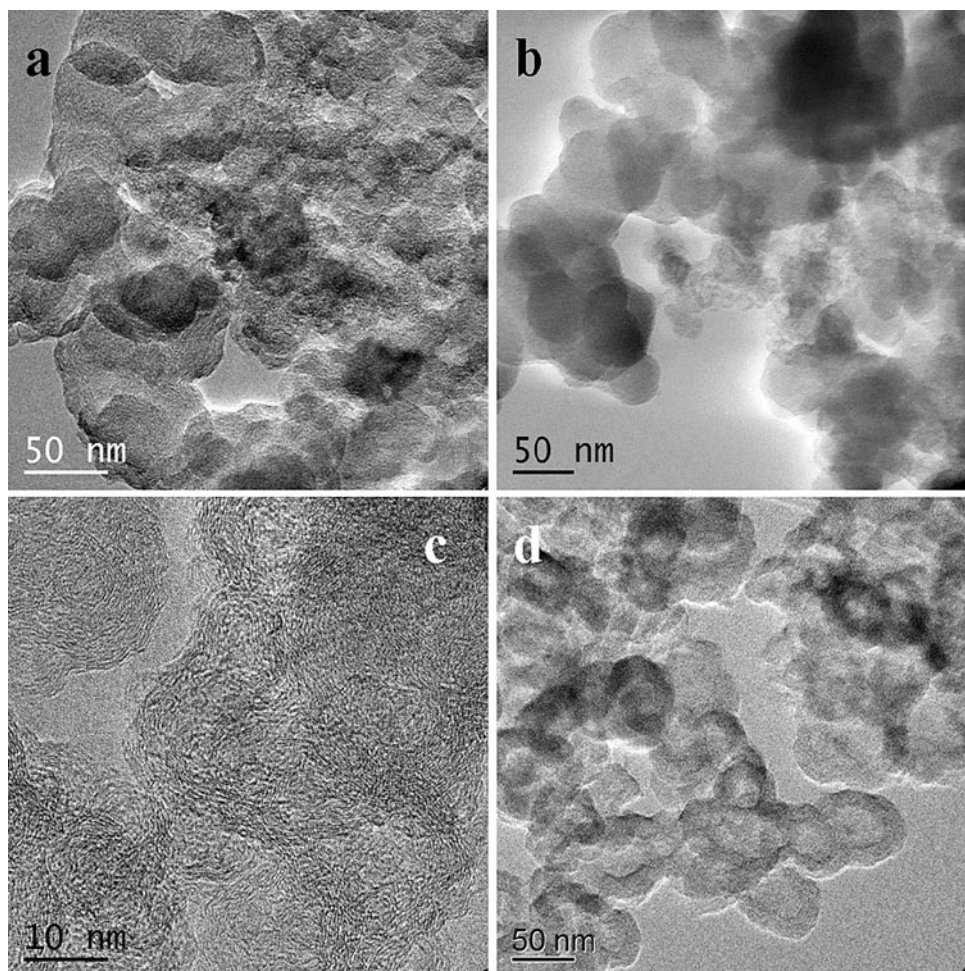
Sample	BET surface area (m ² /g)	Total pore volume (cm ³ /g)	Nb ₂ O ₅ loading (wt%) ^a
Carbon black (CB)	169	0.11	–
Nb/CB-1-DP ^b	175.2	0.25	6.9
Nb/CB-2-DP	149.2	0.76	6.5
Nb/CS-HT ^c	102.9	0.48	8.9

^a Nb₂O₅ loading was determined by burning off the carbon in a TGA in air

^b CB-1 and CB-2 are carbon black functionalized by nitric acid at 80 °C and 120 °C, respectively

^c CS-HT: carbon prepared by hydrothermal synthesis [17]

Fig. 1 TEM images of carbon materials: **a** as-received carbon black; **b** carbon black functionalized in nitric acid at 80 °C; **c** HR-TEM image of carbon black functionalized in nitric acid at 80 °C; **d** carbon black functionalized in nitric acid at 120 °C



oxygenate groups on the carbon surface. The bands at 1,693 and 1,510 cm⁻¹ are ascribed to the C=O and C=C bands, respectively [19, 22] and the bands at 1,800–2,600 cm⁻¹ are ascribed to the C–O or C=O species. Further, although the Nb/CB-2-DP shows a similar FTIR spectrum to Nb/CB-1-DP, the former shows more intense peaks than the latter, this indicates that more functional groups are present on the Nb/CB-2-DP catalyst surface. It is interesting to note that the FTIR spectrum of Nb/CS-HT exhibits completely different bands, in comparison with

both Nb/CB-1-DP and Nb/CB-2-DP. The FTIR spectrum of Nb/CS-HT shows three bands at 1,705, 1,590 and 1,230 cm⁻¹ and no band was found at 1,800–2,800 cm⁻¹. The bands at 1,705 and 1,590 cm⁻¹ are ascribed to the C=O and C=C bands, respectively [23]. The band at 1,230 cm⁻¹ is ascribed to the C–C band [24]. Thus, the FTIR results revealed that a larger amount of functional groups (C=O, C–O and C=C species) were contained on the Nb/CB-1-DP and Nb/CB-2-DP surface and different groups (C=C, C=O and C–C species) were present on the

Fig. 2 SEM/STEM images of Nb/CB-DP prepared by deposition precipitation: **a** and **b** Nb/CB-1-DP; **c** Nb/CB-2-DP; **d** HR-TEM image of Nb/CB-2-DP showing that the niobia particles are amorphous (*red box*)

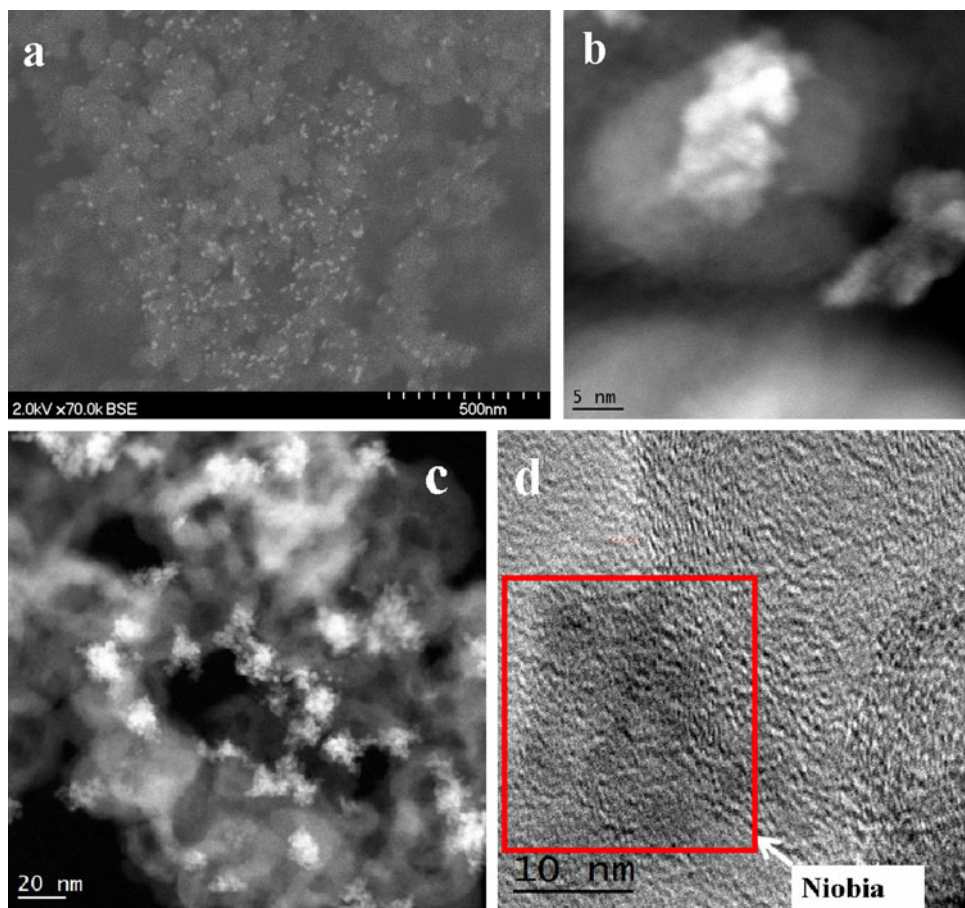
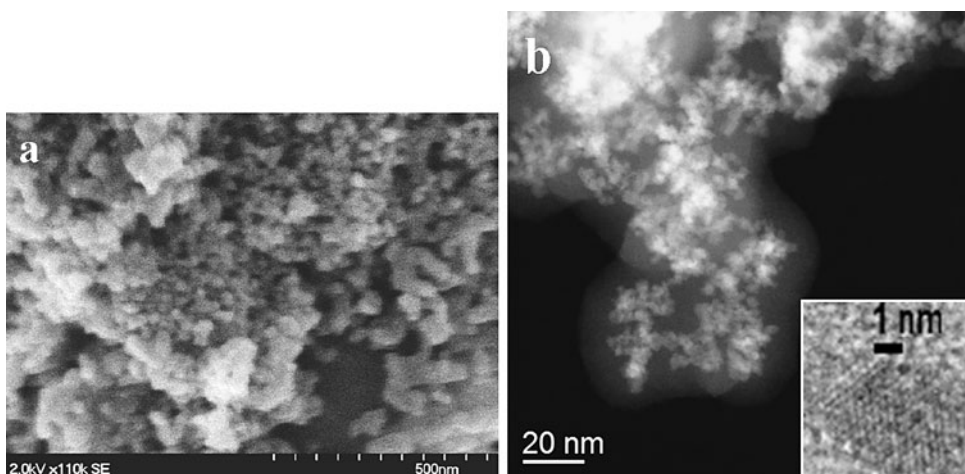


Fig. 3 Electron microscopy of Nb/CS-HT prepared by the DPC method at 200 °C for 12 h: **a** SEM image showing a wide area view; **b** STEM image showing clearly the niobia particles and HR-TEM image showing the lattice fringes of niobia (insert)



Nb/CS-HT surface. This difference can be related to the method of preparation, acid treatment in the case of the CB samples compared with hydrothermal transformation of a sugar followed by pyrolysis in the case of the CS-HT sample.

3.4 TGA Results

The thermal stability of the niobia/carbon catalysts were studied in a flow of N₂ and shown in Fig. 5. For Nb/CB-1-DP, <10 % weight loss was observed when the sample was

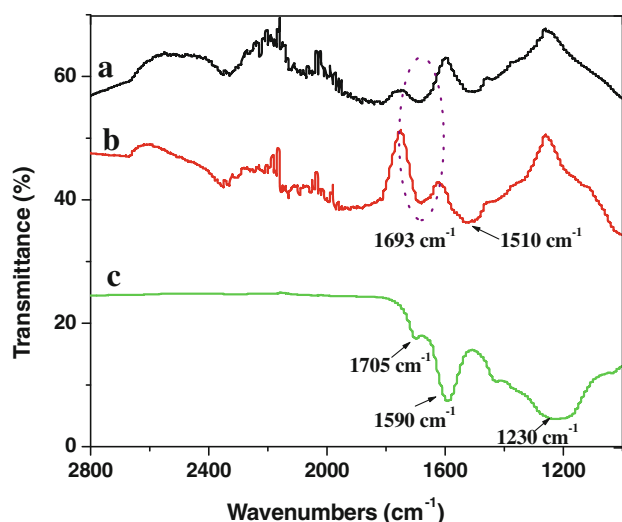


Fig. 4 FTIR spectra of the niobia/carbon catalysts: **a** Nb/CB-1-DP; **b** Nb/CB-2-DP; **c** Nb/CS-DP

heated to 900 °C (Fig. 5a). The DTG curve shows that four weight loss regions are observed and centered at 60, 250, 450 and 700 °C, respectively. The Nb/CB-2-DP catalyst shows a similar weight loss behavior, while a weight loss of 25 % was found when the temperature was increased to 900 °C (Fig. 5b). According to our previous study [19], the peak at 60 °C was ascribed to the release of adsorbed water in the sample and the peak between 300 and 600 °C assigned to the removal of some functional groups on the carbon sample. Thus, the Nb/CB-2-DP exhibited significant greater amounts of surface functional groups, as compared to Nb/CB-1-DP. This agrees well with the FTIR result. For the Nb/CS-HT prepared by DPC, two weight loss peaks are found when it was heated in N₂ (Fig. 5c). The peak at 60 °C was ascribed to the release of adsorbed water in the sample. The peak between 300 and 900 °C assigned to the removal of some functional groups and the decomposition of residual levulinic acid in the catalyst based on NMR [25].

3.5 Catalytic Performance and Hydrothermal Stability

3.5.1 Isopropanol Dehydration in Gas-Phase Reactor

The gas-phase reaction of 2-propanol dehydration was used to probe the nature of the surface acid sites in the niobia/carbon solid acid catalysts. Further, a hydrothermal treatment process in an autoclave at 200 °C for 12 h was used to investigate the hydrothermal stability of the catalyst. The results of 2-propanol dehydration at 180 °C for niobia/carbon catalysts before and after hydrothermal treatment are shown in Table 2. As can be seen, before the treatment in liquid water, all niobia/carbon catalysts showed a

propylene formation rate range of 1.7–2.4 μmol · min⁻¹ · g⁻¹ · Nb. After treatment in liquid water at 200 °C for 12 h, the activity of all catalysts decreased by about 50 %. The higher activity of the Nb/CS-HT catalyst is related to the increased crystallinity of the niobia in this sample, as detected via HR-TEM.

3.5.2 Conversion of D-Glucose to 5-Hydroxymethylfurfural (HMF) in the Biphasic System

The catalytic behavior and the effect of different locations of the niobia/carbon catalysts were investigated in the conversion of D-glucose to 5-hydroxymethylfurfural in a biphasic system (water and sec-butyl phenol). The biphasic system allows the SBP solvent to continuously extract the HMF produced from the aqueous phase into the organic phase, thereby minimizing HMF degradation. We first investigated the locations of the niobia/carbon catalysts in the biphasic system. As can be seen in Fig. 6, the Nb/CB-1-DP was present exclusively in the organic phase (Fig. 6a), while the Nb/CB-2-DP was entirely present in the aqueous phase (Fig. 6c). Because both these catalyst supports are functionalized by nitric acid but at different temperatures and the catalysts are prepared by the same method, the different locations are due to the different degree of hydrophobicity/hydrophilicity on the carbon surface. It is interesting to note that the Nb/CS-HT catalyst was located at the interface between the aqueous and organic phase suggesting it has an intermediate degree of hydrophobicity (Fig. 6b).

The catalytic reactivity of the niobia/carbon catalysts are shown in Table 3. For the niobia catalysts supported on carbon black, the Nb/CB-1-DP shows a glucose conversion of 34 % while the Nb/CB-2-DP shows the highest glucose conversion of 78 %. The higher glucose conversion for Nb/CB-2-DP can be related to the niobia/carbon catalyst and D-glucose being present in the same phase (aqueous phase) thus ensuring intimate contact of reactants and catalyst. The Nb/CS-HT shows the lowest conversion and HMF selectivity since it is located at the interface, leading to a little contact between catalyst and glucose. The HMF yield for the niobia/carbon composites are in the range of 10–20 %, which compares favorably with the 20 % HMF selectivity reported recently on pure niobia catalysts [12]. The niobia/carbon composite developed in this work are more hydrothermally stable than pure niobia [26]. Moreover, although both the above reactions are acid catalyzed, the dehydration reactivity of niobia/carbon catalysts in the liquid phase does not scale with the dehydration of isopropanol in the vapor phase. This is because we are conducting a biphasic reaction and the location of the catalyst, in the aqueous phase, organic phase or the interface, played a bigger role than the intrinsic catalytic activity.

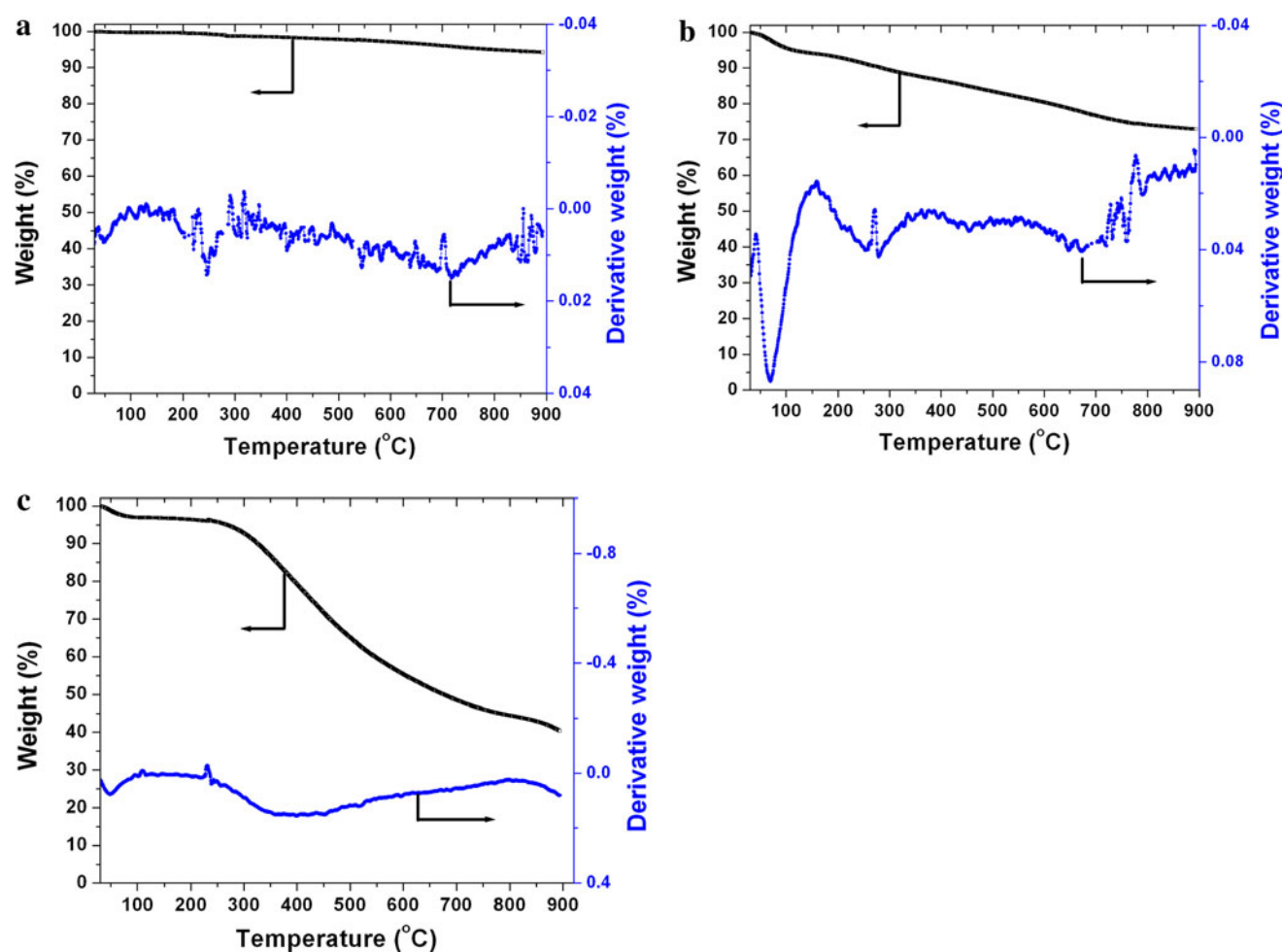


Fig. 5 TGA and DTG data for niobia/carbon catalysts in N_2 : **a** Nb/CB-1-DP; **b** Nb/CB-2-DP; **c** Nb/CS-HT

Table 2 Reactivity for the dehydration of 2-propanol before and after hydrothermal treatment in liquid water at 200 °C for 12 h

Catalyst	Propylene formation rate ($\mu\text{mol min}^{-1} \text{g}^{-1}\text{Nb}$)	
	Before treatment in liquid water	After treatment in liquid water
Nb/CS-HT	2.4	1.1
Nb/CB-1-DP	1.7	0.74
Nb/CB-2-DP	1.9	0.81

4 Conclusions

Nano-structured niobia/carbon catalysts were prepared by two different preparation methods. The niobia/carbon black catalysts prepared by deposition–precipitation (DP) show niobia clusters of 20 nm, which are comprised of amorphous niobia particles of 3 nm. A niobia/carbon catalyst (Nb/CS–HT) prepared by deposition precipitation-carbonization (DPC) shows crystalline niobia particles with a size of 8 nm. The different catalysts have different degrees

of hydrophilicity, hence they are located in different locations in the biphasic water/sec-butyl phenol system. The niobia/carbon catalyst (Nb/CB-1-DP) prepared by DP using a carbon black pretreated in nitric acid at 80 °C was present in the organic phase, while the niobia/carbon catalyst (Nb/CB-2-DP) prepared by DP using the carbon black pretreated in nitric acid at 120 °C was mainly located in the aqueous phase. The Nb/CS–HT was found to locate at the interface between the organic and aqueous phases. The different locations for the niobia/carbon catalysts were found to significantly affect the catalytic behavior in the conversion of D-glucose to 5-hydroxymethylfurfural resulting from their different extent of contact with the glucose. The Nb/CB-2-DP shows the highest D-glucose conversion (twofold than the others dispersed in interface or organic phase), which was ascribed to both niobia/carbon catalyst and D-glucose distributed in the same phase (aqueous phase) that ensuring complete contact of reactant and catalyst. The reactivity did not scale with the conversion of isopropanol in the vapor phase, a reaction that would probe the nature of the acid sites. This is because the

Fig. 6 Photographs of the locations of niobia/carbon catalysts dispersed in sec-butyl phenol/water ($v/v = 2$): **a** organic phase; **b** interface; **c** aqueous phase

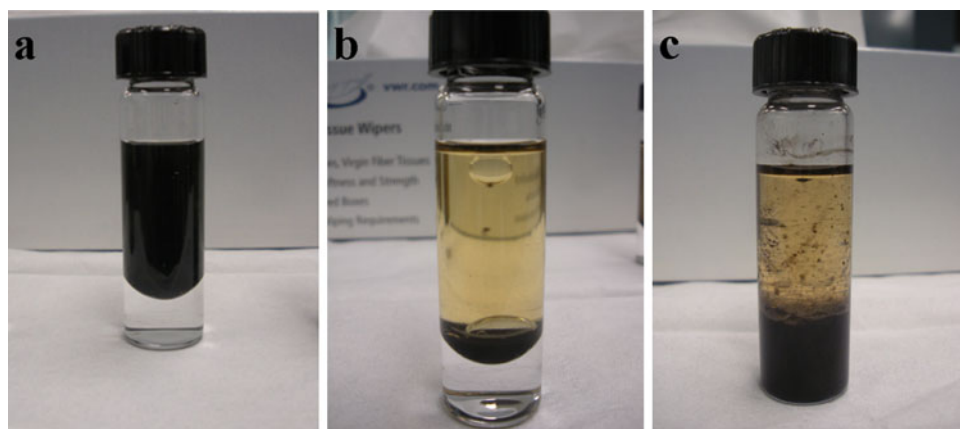


Table 3 Performance of niobia/carbon catalysts in the conversion of D-glucose to 5-hydroxymethylfurfural (HMF)

Catalyst	Conversion (%)	Selectivity (%)	Yield (%)	Location
Nb/CS-HT	33	34	11	Interface
Nb/CB-1-DP	34	52	18	Organic phase
Nb/CB-2-DP	78	26	20	Aqueous phase

Reaction conditions: 5wt % D-glucose in water saturated with NaCl, reaction temperature of 170 °C, organic to aqueous mass ratio of two, reaction time of 2 h

location of the catalyst played a bigger role than intrinsic catalytic activity. The results suggest that the acid sites on the niobia catalysts are not ideally suited for the glucose conversion reaction, and the ratio of Lewis to Bronsted acid need to be further tuned to achieve optimal reactivity.

Acknowledgments This work is supported by the NSF Engineering Research Center for Biorenewable Chemicals (CBiRC) supported by award number EEC 0813570. The XRD facilities used in this work were supported by NSF MRI grant CBET 0960256. We thank Dr. Hien Pham for N₂ physisorption measurements.

References

- Davis SE, Zope BN, Davis RJ (2012) *Green Chem* 14:143
- Buntara T, Noel S, Phua PH, Melián-Cabrera I, de Vries JG, Heeres HJ (2011) *Angew Chem Int Ed* 50: 7083
- Chidambaram M, Bell AT (2010) *Green Chem* 12:1253
- Huber GW, Chheda JN, Barrett CJ, Dumesic JA (2005) *Science* 308:1446
- Roman-Leshkov Y, Barrett CJ, Liu ZY, Dumesic JA (2007) *Nature* 447:982
- Qi X, Watanabe M, Aida TM, Smith RL (2012) *Bioresource Technol* 109:224
- Zhao H, Holladay JE, Brown H, Zhang ZC (2007) *Science* 316:1597
- Crossley S, Faria J, Shen M, Resasco DE (2010) *Science* 327:68
- Wang J, Ren J, Liu X, Xi J, Xia Q, Zu Y, Lu G, Wang Y (2012) *Green Chem* 14:2506
- Wang T, Pagán-Torres Y, Combs E, Dumesic JA, Shanks B (2012) *Top Catal* 55:657
- Huang R, Qi W, Su R, He Z (2010) *Chem Commun* 46:1115
- Nakajima K, Baba Y, Noma R, Kitano M, N. Kondo J, Hayashi S, Hara M (2011) *J Am Chem Soc* 133:4224
- Fan C, Guan H, Zhang H, Wang J, Wang S, Wang X (2011) *Biomass Bioenergy* 35:2659
- De S, Dutta S, Patra AK, Bhaumik A, Saha B (2011) *J Mater Chem* 21:17505
- Nikolla E, Román-Leshkov Y, Moliner M, Davis ME (2011) *ACS Catal* 1:408
- Pham HN, Anderson AE, Johnson RL, Schmidt-Rohr K, Datye AK (2012) *Angew Chem Int Ed* 51:13163
- Xiong HF, Pham HN, Datye AK (2013) *J Catal.* doi:10.1016/j.jcat.2013.03.007
- Rodríguez-reinoso F (1998) *Carbon* 36:159
- Xiong HF, Moyo M, Motchelaho MAM, Jewell LL, Coville NJ (2010) *Appl Catal A Gen* 388:168
- Pagán-Torres YJ, Wang T, Gallo JMR, Shanks BH, Dumesic JA (2012) *ACS Catal* 2:930
- Román-Leshkov Y, Dumesic JA (2009) *Top Catal* 52:297
- Moyo M, Motchelaho MAM, Xiong HF, Jewell LL, Coville NJ (2012) *Appl Catal A Gen* 413–414:223
- Titirici MM, Thomas A, Yu S-H, Müller J-O, Antonietti M (2007) *Chem Mater* 19:4205
- Shin Y, Wang L-Q, Bae I-T, Arey BW, Exarhos GJ (2008) *J Phys Chem C* 112:14236
- Baccile N, Laurent G, Babonneau F, Fayon F, Titirici M-M, Antonietti M (2009) *J Phys Chem C* 113:9644
- Pagán-Torres YJ, Gallo JMR, Wang D, Pham HN, Libera JA, Marshall CL, Elam JW, Datye AK, Dumesic JA (2011) *ACS Catal* 1:1234